Available online at www.sciencedirect.com
ScienceDirect
Journal of Nuclear Materials 356 (2006) 105–111
journal of nuclear materials
www.elsevier.com/locate/jnucmat

Microstructure of the F82H martensitic steel irradiated in STIP-II up to 20 dpa

X. Jia, Y. Dai *

Paul Scherrer Institut, CH-5232 Villigen, PSI, Switzerland

Abstract

The F82H martensitic steel was irradiated in the STIP-II experiment in SINQ up to 20 dpa in a temperature range of 110–400 °C. Transmission electron microscope observations have been performed to study the effects of radiation on the microstructure. The results show that at $\leqslant$350 °C, the size of defect clusters or dislocation loops increases with both dose and temperature. The density of defect clusters or dislocation loops increases with increasing dose but decreases with temperature. A high-density of small He bubbles are visible in samples irradiated at $\geqslant$165 °C with $\geqslant$750 appm He. The bubble size increases while the density decreases with increasing irradiation temperature. These results agree with the previous observations of STIP-I specimens. In a specimen irradiated to 20.3 dpa with 1800 appm He at 400($\pm$50) °C, large voids up to 50 nm in size were detected. The bubbles showed a bimodal size distribution. The martensite lath structure was almost completely removed by radiation. Meanwhile, the $M_{23}C_6$ precipitates along prior martensite lath and austenite boundaries disappeared and new $M_{23}C_6$ precipitates were formed in the matrix of new grains. In all cases, no obvious segregation of bubbles on grain boundaries was observed. However, it was detected that helium bubbles locate preferentially at pre-existing dislocations.

1. Introduction

Martensitic steels are candidate materials for the first wall blanket of fusion reactors and the liquid metal containers of high power spallation targets [1,2]. The F82H low-activation martensitic steel shows relatively low shifts in ductile-to-brittle-transition temperature (DBTT) after neutron irradiation [3], and therefore the F82H steel has been selected as one of main materials irradiated and studied in the SINQ target irradiation program (STIP).

The STIP is one of the key activities aimed at studying radiation damage in structural materials produced by high-energy protons and spallation neutrons [4]. Presently, numerous results have been reported from the first STIP experiment (STIP-I), showing many interesting observations about the effects of high energy protons and neutrons on the microstructure and mechanical properties of different materials such as ferritic/martensitic steels, austenitic stainless steels and Al-alloys [5–8].

A series of studies have been conducted on the microstructure of the F82H steel irradiated in STIP-I. In STIP-I, the maximum irradiation dose of steel samples was limited to about 12 dpa with 1100 appm helium and the irradiation temperature

* Corresponding author. Tel.: +41 56 310 4171; fax: +41 56 310 4529.
E-mail address: yong.dai@psi.ch (Y. Dai).

0022-3115/$ - see front matter © 2006 Elsevier B.V. All rights reserved.
doi:10.1016/j.jnucmat.2006.05.006

Table 1
Irradiation conditions and TEM measurement results

Specimen	Dose (dpa)	He (appm)	T_{irr} (°C)	Defect size (nm)	Defect density (m^{-3})	Bubble size (nm)	Bubble density (m^{-3})
K^1	15.7	1130	165 ± 15	4.9	3.82×10^{22}	0.9	–
K^2	10.0	660	112 ± 10	3.7	3.17×10^{22}	–	–
K^3	20.3	1800	400 ± 50	8.5	2.88×10^{22}	5.0	2.48×10^{23}
K^5	7.2	550	145 ± 15	2.7	3.14×10^{22}	–	–
K^a	18.6	1570	350 ± 30	9.5	1.38×10^{22}	3.3	3.30×10^{23}
K^b	9.8	750	185 ± 20	4.2	4.03×10^{22}	0.9	3.76×10^{23}
K^c	5.5	375	115 ± 10	2.8	2.43×10^{22}	–	–

was up to 360 °C. In STIP-II, which was performed in 2000 and 2001 in SINQ Target-4, more than 2000 samples from different materials were irradiated to up to ~20 dpa (in steels) and 1800 appm He at ⩽430 °C [9]. The post-irradiation examination (PIE) is being conducted. The present work shows some recent results of microstructural observations on the F82H steel irradiated up to 20.3 dpa at irradiation temperatures ⩽400 °C.

2. Experimental

The STIP-II irradiation was started on the 20th of March, 2000 and interrupted on the 23rd of December. After a long break it was started again on the 15th of May and finally ended on the 23rd of December, 2001. The total irradiation time was about 16 months. In the nine months of 2000, a proton charge of 5.56 Ah was received, and in the seven months of 2001, another 4.47 Ah was reached, which gave a total proton charge of 10.03 Ah. The variation of the irradiation temperature during these two periods was as great as 20% of the averaged temperature values. The temperature values used in this report are the average values. The irradiation dose, helium and hydrogen concentrations were calculated with the MCNPX code. But the helium and hydrogen concentrations were corrected with measurements. More detailed information can be found in [9,10]. As the measurements showed that the hydrogen retention in irradiated steels decreased rapidly with increasing irradiation temperature and was very low (<10% of the calculated values) in samples irradiated at above about 200 °C, the hydrogen content is not indicated in this paper.

The F82H steel used in this work is the same material as used in the previous studies with a composition in wt%: 7.65 Cr, 2 W, 0.16 Mn, 0.16 V, 0.02 Ta, 0.11 Si and 0.09 C with balance Fe [11]. TEM discs of the F82H steel were irradiated in STIP-II to doses ranging from 5.5 dpa to 20 dpa. Table 1 summarizes the irradiation dose and temperature of the samples.

The preparation of TEM samples was optimized by using the 1 mm technique, namely 1 mm discs were punched from original 3 mm TEM discs to minimize radioactivity and magnetic effects on observations [12]. The TEM investigation was performed in a JEOL 2010 type transmission electron microscope operated at 200 kV. The most often used image conditions were bright field (BF) and weak beam dark-field (WBDF) at g ($5g$–$6g$), $g = 110$ near $z = 111$. BF micrographs were used for counting He bubbles and WBDF micrographs of g ($5g$) were used for quantifying defect clusters.

3. Results and discussion

Fig. 1 shows the WBDF images of the defect structure in samples irradiated up to 15.7 dpa at irradiation temperatures, ⩽260 °C. The results agree well with our previous observations on the same steel irradiated in STIP-I at similar temperatures [5,8], namely the main feature is the formation of small defect clusters. The mean defect size and the defect density both increase with increasing irradiation dose. The size also increases with temperature but the density decreases.

Due to the resolution limit of the TEM, helium bubbles could only be seen when they grow to size of about 1 nm. The previous work showed that helium bubbles became to be visible at irradiation temperatures above about 170 °C with about 500 appm He in F82H [5]. In the present work, bubbles were observed in a sample irradiated to 9.8 dpa/750 appm He at about 185 °C, as shown in Fig. 2(a) and (b) in the over-focused and under-focused image conditions, respectively. A high-density small helium bubbles with a mean size about 1 nm distrib-

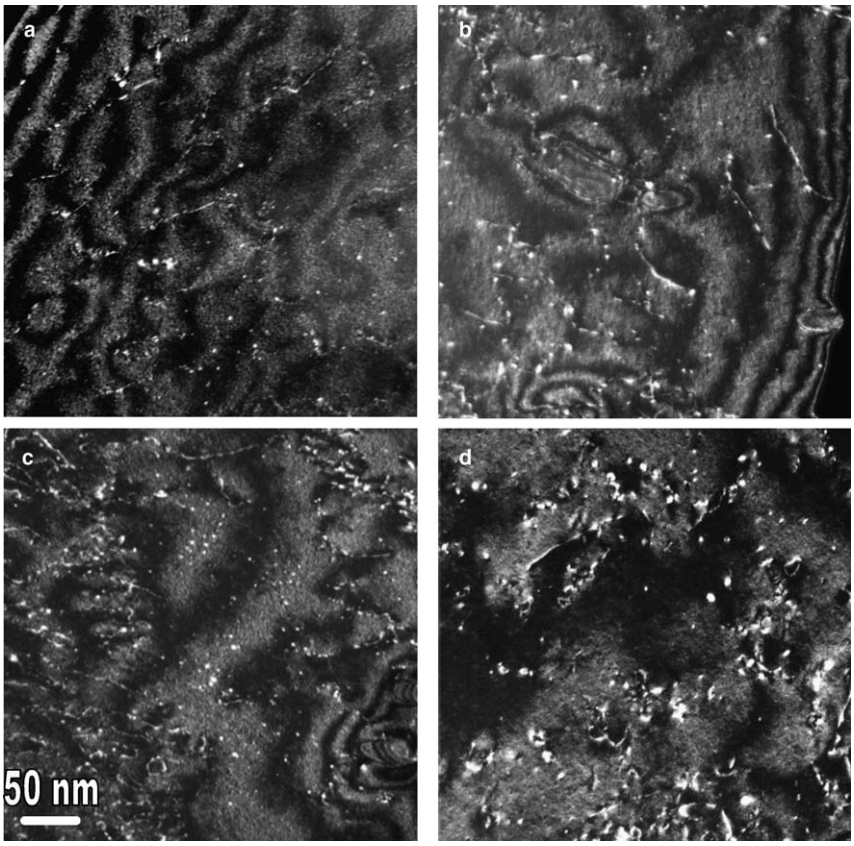

Fig. 1. WB images showing the defect cluster structure of F82H samples irradiated at different conditions: (a) K^c, 5.5 dpa/115 °C, (b) K^4, 7.3 dpa/145(±15) °C, (c) K^2, 10.0 dpa/112(±10) °C and (d) K^1, 15.7 dpa/165(±15) °C. The image condition is g (5g) with $g = \mathbf{110}$ for all.

uted homogeneously in the matrix. With increasing irradiation temperature, irradiation dose and helium concentration, the mean size of the helium bubbles increased. In Fig. 2(c) and (d), two BF images show the bubble structure of a sample irradiated to 18.6 dpa/1570 appm He at 350 °C. The bubbles had a mean size about 3 nm and distributed preferentially along pre-existing dislocation lines and precipitate–matrix boundaries.

At the highest irradiation dose 20.3 dpa/1800 appm He and temperature 400 °C, the distribution of helium bubbles in the matrix showed clearly bimodal behaviour (Fig. 2(e) and (f)) and voids up to 50 nm appeared. Obvious denuded zone of bubbles nearby grain boundaries and abundant bubbles on grain boundaries were not observed in specimens of martensitic steels irradiated in STIP at $\leqslant$400 °C. The size distributions of helium bubbles in these three irradiation conditions are presented in Fig. 3. With increasing irradiation temperature, the bubble density decreased and showed a large drop at 400 °C, as shown in Fig. 4.

An interesting result is that large bubbles (or voids) were observed in some areas having relatively dense precipitates, as can be seen in Fig. 2(e) and (f). This phenomenon is not yet understood. One possible reason can be that the dense precipitates changed significantly the local matrix composition. Another reason can be the temperature excursion. Further investigations are on going to check these explanations.

Maziasz et al. [13] reported that after irradiation in HFIR to ~38 dpa and ~32 appm He at 400 °C, very fine helium bubbles (about 2–5 nm, 1.6 to 3.5×10^{22} m^{-3}) and large voids (7–30 nm, 2.2 to 2.5×10^{21} m^{-3}) were detected in the 9Cr1MoVNb steel. Meanwhile, in the Ni-doped 9Cr1MoVNb–2Ni steel irradiated in the same irradiation condition but with 410 appm He the formation of bubbles and voids was more uniform and significantly denser than those in the non doped 9Cr1MoVNb steel. The comparison suggested that helium increases bubble and void formation in martensitic/ferrite steels. The swelling due to helium bubbles and voids

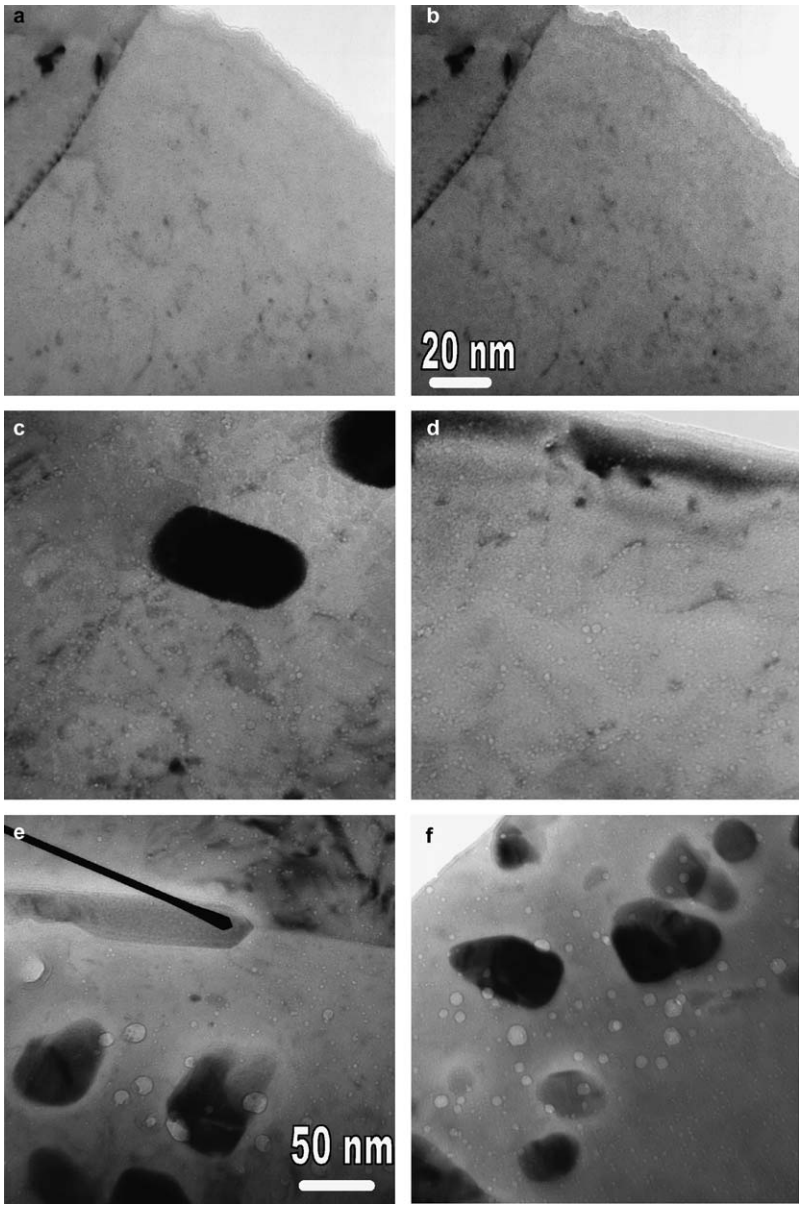

Fig. 2. Helium bubble structure in the samples K^b, K^a and K^3 irradiated in SINQ target-4. (a) and (b) for K^b, 9.8 dpa/185(±20) °C, in over-focused and under-focused image conditions, respectively; (c) and (d) for K^a, 18.6 dpa/350(±30) °C and (e) and (f) for K^3, 20.3 dpa/400(±50) °C.

was ~0.2% in the 9Cr1MoVNb steel and 0.3–0.4% in 9Cr1MoVNb–2Ni steel. Although ferritic/martensitic steels were often reported to exhibit good resistance to void swelling, a recent reanalysis of some fast reactor swelling data suggested that the post-transient swelling rate might be higher than previously reported [14]. There was also some evidence for enhanced cavity swelling in the F82H steel irradiated to doses of about 40 dpa with fission neutrons or ions at fusion-relevant levels of helium [15–17]. In the present work, a swelling of about 3% was calculated for the sample irradiated to 20.3 dpa/1800 appm He at 400 °C. It implies that ferritic/martensitic steels may exhibit large, enhanced swelling at high helium concentrations and high dpa levels.

The helium production rate in steel samples irradiated in STIP varies from 50 to 90 appm/dpa [9], which is much higher than that of neutron irradiation in most fast and thermal reactors, about

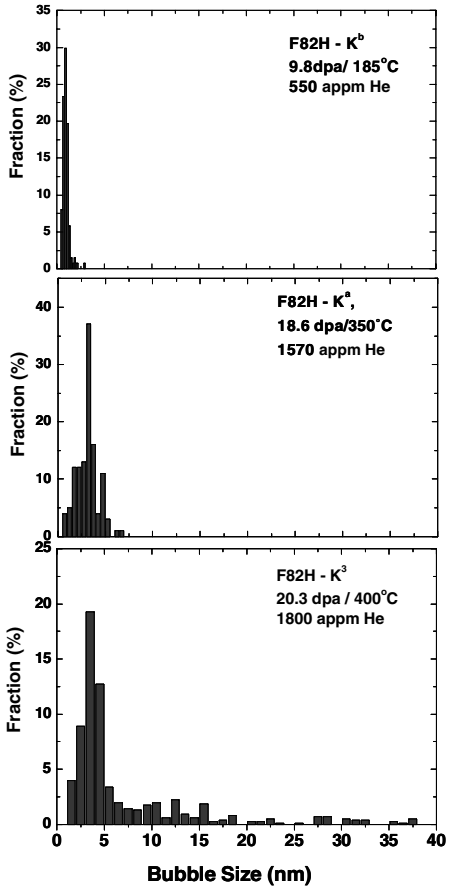

Fig. 3. Size distribution of helium bubbles in three samples, K^a, K^b and K^3. The irradiation conditions are indicated in the plots.

1 appm He/dpa or less. The high helium production rate provides more nucleation sites for bubbles, particularly at lower temperatures where helium atoms are less mobile. This results in a high density of small bubbles as detected in the samples of martensitic steels irradiated in STIP at temperatures between 200 and 400 °C [5,8].

Before irradiation, the as-tempered grain and sub-grain structure in the F82H steel consists of large prior austenite boundaries and packet boundaries surround groups of martensite laths with a similar orientation, and $M_{23}C_6$ precipitates locate mostly along prior austenite boundaries and martensite lath boundaries [5,8]. Our previous studies demonstrated that after irradiation to about 12 dpa at 360 °C, no change occurred in the original martensite lath structure and precipitate structure in the F82H steel [5]. However in the present work, it was observed that both lath and precipitate structures were changed after irradiation to 20.3 dpa at 400(±50) °C. The martensite lath structure was almost completely removed. At the same time, the $M_{23}C_6$ precipitates along prior austenite boundaries and martensite lath boundaries disappeared, while new $M_{23}C_6$ precipitates formed inside the matrix, as shown in Fig. 5. In neutron irradiations, tempered martensite lath structure of 7–9 Cr% JLF steels (similar to the F82H steel) was stable after irradiation to 35 dpa at 410 °C. Some recovery of martensite lath structure was observed at 460 °C with a slight coarsening or agglomeration

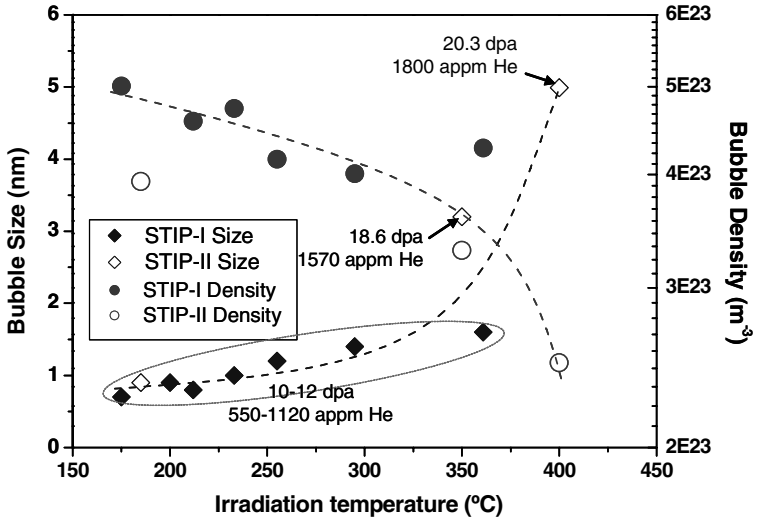

Fig. 4. Temperature dependence of the mean size and the density of helium bubbles. The irradiation dose and helium concentration values are indicated at bubble size data points.

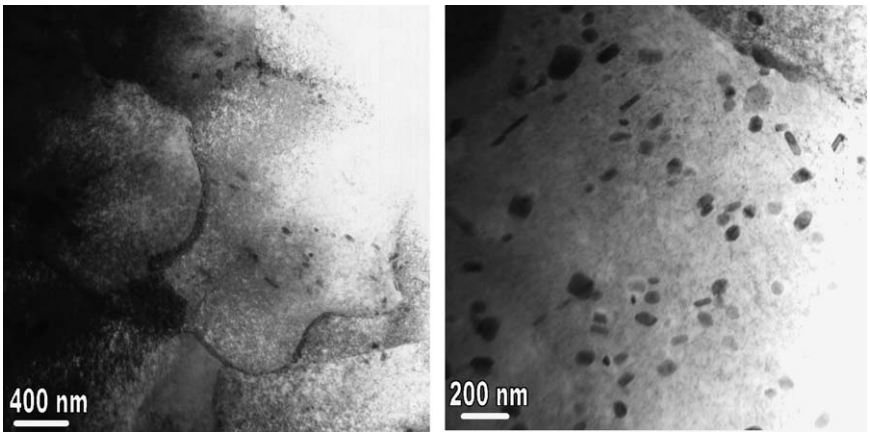

Fig. 5. BF image showing the absence of martensite lath structure and $M_{23}C_6$ precipitates along the lath boundaries. New $M_{23}C_6$ precipitates have formed inside the matrix during irradiation.

of precipitates along lath or sub-grain boundaries. Above 520–550 °C, full recovery of martensite lath structure and disappearance of precipitates along boundaries were observed [17,18]. As for the present specimen irradiated to 20.3 dpa, it was once irradiated at about 560 °C for about 20 h due to slightly focused proton beam at the target. This short temperature excursion occurred after seven months and followed by another nine months of irradiation. Although this high temperature period was not so long, it could also be the reason for the significant changes of lath and precipitate structure in this specimen. In addition, the large bubbles or voids observed in this specimen might be attributed to

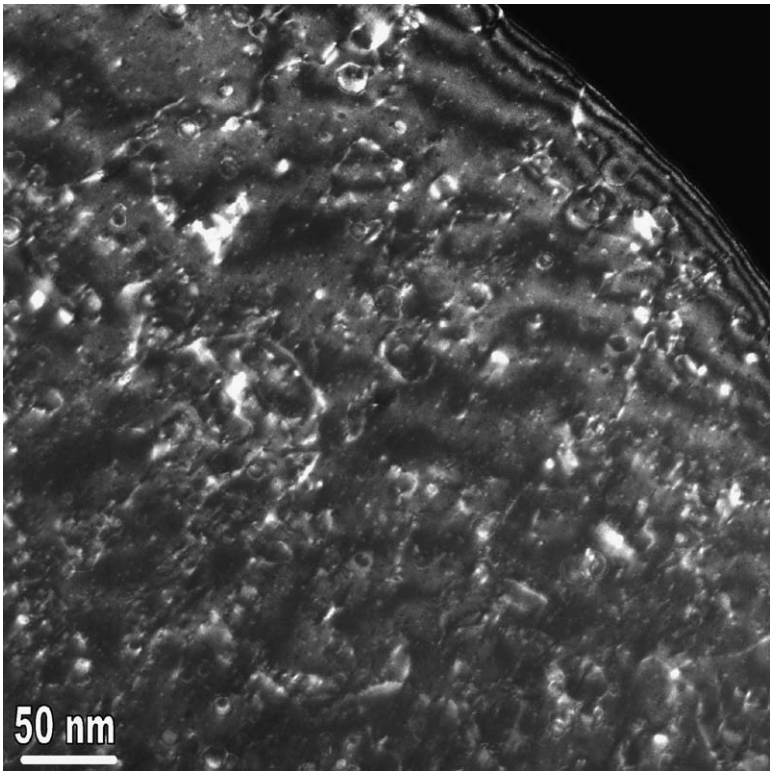

Fig. 6. WBDF image showing defect cluster structure in a sample irradiated to 20.3 dpa at 400(±50) °C. The image condition is g (5g) with $g = \mathbf{110}$.

the same reason. As for other specimens, they also experienced the temperature excursion at the same time, but at lower temperature levels (<490 °C). Therefore, it is reasonable that no such changes were detected in them.

Fig. 6 shows a WBDF image of samples irradiated to 20.3 dpa at 400 °C. We can see that the density of defect clusters (mostly are Frank interstitial loops) is still very high. This seems not consistent with the previous observation which shows the defect density decreasing rapidly after irradiation at temperatures higher than about 300 °C. It can be explained by the disappearance of martensite lath structure after the high temperature excursion. As martensite lath boundaries are strong sinks for irradiation produced interstitials and vacancies in the steel, after they were removed, the density of defect clusters could increase significantly.

4. Conclusions

The F82H steel was irradiated in STIP-II to up to 20 dpa in a nominal temperature range of 110–400 °C. TEM observations showed that:

1. At temperature $\leqslant$350 °C, the size of defect clusters or dislocation loops increased with dose and temperature. The density of defect clusters or dislocation loops increased with dose but decreased with temperature. A high-density of small He bubbles were visible in samples irradiated at $\geqslant$165 °C with $\geqslant$750 appm He. The bubble size increased while the density decreased with increasing irradiation temperature. These results agree with the previous microstructural observations of STIP-I specimens.
2. In a specimen irradiated to 20.3 dpa/1800 appm He at 400($\pm$50) °C, bubbles (or voids) up to 50 nm large were detected. The bubbles showed a bimodal size distribution. The martensite lath structure were almost completely removed. Meanwhile, the $M_{23}C_6$ precipitates along martensite lath and prior austenite boundaries disappeared and new $M_{23}C_6$ precipitates formed inside the matrix of new grains. Such a significant change in microstructure might be attributed to the high temperature excursion of 20 h at 560 °C during irradiation.
3. In all specimens, including those of STIP-I, no obvious abundant bubble formation in grain boundaries was observed. However, it was detected that helium bubbles locate preferentially at pre-existing dislocations.

Acknowledgements

This work was included in the SPIRE (Irradiation effects in martensitic steels under neutron and proton mixed spectrum) subprogram of the European 5th Framework Program and was supported by Swiss Bundesamt fuer Bildung und Wissenchaft.

References

[1] R.L. Klueh, in: Proceedings of 1st International Workshop on Spallation Materials Technology, 23–25 April 1996, Oak Ridge, p. 3.3.
[2] Y. Dai, in: Proceedings of ICANS-XIII and ESS-PM4, 11–19 October 1995, PSI, p. 604.
[3] A. Kohyama, A. Hishinuma, D.S. Gelles, R.L. Klueh, W. Dietz, K. Ehrlich, J. Nucl. Mater. 233–237 (1996) 138.
[4] Y. Dai, G. Bauer, J. Nucl. Mater. 296 (2001) 43.
[5] X. Jia, Y. Dai, M. Victoria, J. Nucl. Mater. 305 (2002) 1.
[6] Y. Dai et al., J. Nucl. Mater. 318 (2003).
[7] Y. Dai et al., J. Nucl. Mater. 343 (2005).
[8] X. Jia, Y. Dai, J. Nucl. Mater. 318 (2003) 207.
[9] Y. Dai, X. Jia, R. Thermer, D. Hamaguchi, K. Geissmann, E. Lehmann, H.P. Linder, M. James, F. Groeschel, W. Wagner, G.S. Bauer, J. Nucl. Mater. 343 (2005) 33.
[10] Y. Dai, Y. Foucher, M.R. James, B.M. Oliver, J. Nucl. Mater. 318 (2003) 167.
[11] Y. Kohno, D.S. Gelles, A. Kohyama, M. Tamura, A. Hishinuma, J. Nucl. Mater. 191–194 (1992) 868.
[12] R. Schäublin, M. Victoria, J. Nucl. Mater. 283–287 (2000) 339.
[13] P.J. Mazisaz, R.L. Klueh, J.M. Vitek, J. Nucl. Mater. 141–143 (1986) 929.
[14] F.A. Garner, M.B. Toloczko, B.H. Sencer, J. Nucl. Mater. 276 (2000) 123.
[15] E. Wakai, N. Hashimoto, Y. Miwa, J.P. Robertson, R.L. Klueh, K. Shiba, S. Jistukawa, J. Nucl. Mater. 283–287 (2000) 799.
[16] E. Wakai, K. Kikuchi, S. Yamamoto, T. Aruga, M. Ando, H. Tanigawa, T. Taguchi, T. Sawai, K. Oka, S. Ohnuki, J. Nucl. Mater. 318 (2003) 267.
[17] Y. Katoh, M. Ando, A. Kohyama, J. Nucl. Mater. 323 (2003) 251.
[18] Y. Kohno, A. Kohyama, M. Yoshino, K. Asakura, J. Nucl. Mater. 212–215 (1994) 707.